

4 The Effect of Ureteric Stents on Urine Flow

Linda Cummings, Nottingham; Andy Gibson, Cambridge; Stuart Graham, UCL; Peter Howell, Oxford; Paul Huggins, Cambridge; David Riley, Nottingham; Michael Simmonds, Cambridge; Sarah Waters, Jonathan Wattis, Nottingham & Matt Williams, Charing Cross Hospital.

4.1 Introduction

The urinary tract is a conduit, storage and modification system for urine excreted by ultrafiltration from the kidney's parenchyma. It is a dynamic and flexible system, able to handle widely differing flows of fluid through it with comparative ease. The urine is conveyed from the kidney to the bladder via a long thin tube called the ureter. Urine produced is supersaturated, but in normal individuals, inhibitors of crystallisation keep it in a liquid state. Urine entering the bladder is stored at low pressure until voiding is achieved. Rhythmic coordinated contractions of the ureter (peristalsis) push urine down the ureter, and anatomical considerations stop urine returning from the bladder to the kidney.

Unfortunately blockage of the system may occur. This may be from the inside, causes for which include stones, cancers and fibrous bands (strictures) or from the outside, for example overlying fibrosis, bowel tumours, and accidental damage during surgery. The result of this obstruction is increased back pressure on the kidney which, if left untreated, will eventually cause it to fail. A blocked system may get infected, and this can very quickly become life-threatening.

Obstruction is treated, if possible, by removing the obstruction, or repairing around it, but if this is not possible, the obstruction must be relieved. This may be done by direct drainage of the kidney (a nephrostomy) or via the insertion of a plastic tube called a *stent*. For some obstructions stents have to be left *in situ* permanently, but over time they can crust up with crystalline deposits of salts in solution in the urine, a process known as encrustation. This can be painful, cause further blockage, and may necessitate an open operation to remove the crusted stents. Encrustation occurs mainly in areas of urine stasis, *i.e.* the renal pelvis and the bladder.

Anatomical and Physiological considerations

The *renal pelvis* is a funnel-shaped collapsible collecting area for urine generated in the kidney. In the unstented state the renal pelvis has a resting pressure of about 4cm H₂O. When stented this rises to approximately 20cm H₂O. In humans the renal pelvis is rarely empty, *i.e.* some pooling of urine occurs.

The *ureter* is a urothelium-lined muscular tube connecting the renal pelvis to the bladder. In the unstented state, peristaltic waves run down the ureter from a pacemaker centre in the renal pelvis. This happens four to six times a minute, one wave taking approximately twelve seconds to reach the bladder. The presence of a stent abolishes peristalsis. The ureter is approximately 25cm long and has variable width, being approximately 5mm across the lumen. This tends to be slit-like or lobular in cross-section, unless a fluid bolus is passing through. It is narrowest at the pelvi-ureteric junction (PUJ), the vesico-ureteric junction (VUJ), and half-way down where it crosses the pelvic brim.

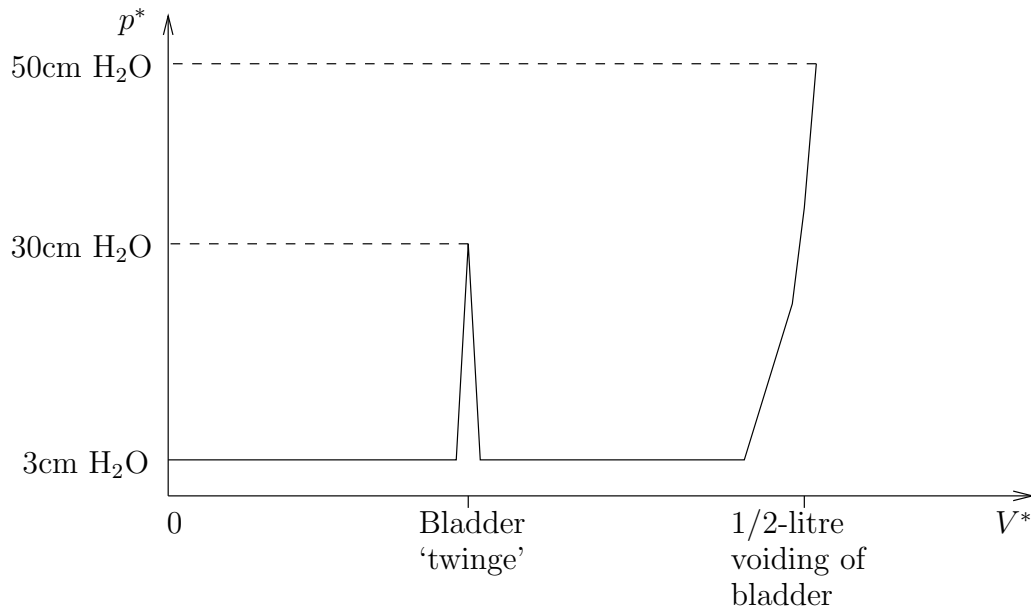


Figure 1: Pressure-volume relationship for the bladder, showing that pressure is independent of volume except on voiding (when it rises to 50cm H₂O) and at twinges (when it rises to 30cm H₂O).

The *vesico-ureteric junction* or VUJ is where the ureter and bladder meet. The ureter tunnels obliquely through the wall of the bladder such that a rise in bladder pressure tends to shut the tube, protecting the kidney from pressure fluctuations. The stent reduces this tendency, as the lower end passes through the VUJ.

The *bladder* is a highly distensible bag that stores and modifies urine. It has a highly compliant wall that keeps bladder pressure low (2–3cm H₂O) excluding the pressure of abdominal contents. Only when almost full (or when the bladder undergoes a short contraction called a ‘twinge’) does the pressure begin to rise (see figure 1). This tells the cerebral cortex that voiding is needed. On voiding, pressures up to 50cm H₂O may be generated. Clinically, a number of different *stent* designs are available for use within the ureter: ‘double-J’ stents made of polymers, which extend the entire length of the ureter, and a range of shorter metal stents which are positioned at the blockage site within the ureter. In this report we consider only one specific design: the double-J (or JJ) stent. This is a polymer tube, which is usually punctuated with holes. It has an internal diameter of about a millimetre. The stent is about 25cm long with additional curls at either end so it doesn’t migrate up into the kidney, or fall out into the bladder. It is relatively pliable longitudinally (‘floppy’) but difficult to compress radially. The lower curl of a stent sits on a sensitive part of the bladder called the trigone. This causes irritation, leading to pressure rises up to 20–30cm H₂O due to muscle contraction.

Urine is produced in a normal kidney at about 1ml min⁻¹. In disease states such as diabetes insipidus, it may reach 8ml min⁻¹. Urine is mainly water, and has similar viscosity and flow characteristics. It contains some salts, urea and a little protein (mainly immunoglobulins). Bladder urine is modified, with concentration and constituent changes happening.

In ordinary function, during voiding, or when the bladder undergoes a ‘twinge’, the VUJ contracts and closes, so that urine cannot travel back up the ureter from the bladder.

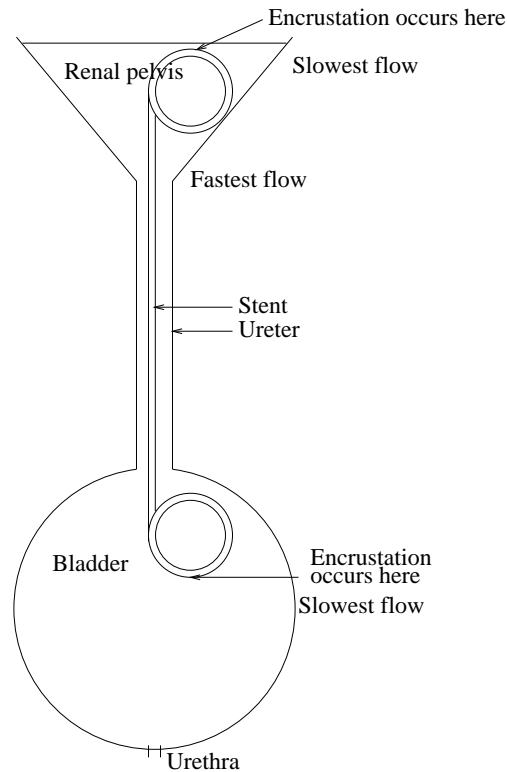


Figure 2: Schematic showing current design and where encrustation occurs.

When stented, however, the VUJ cannot close, because the stent holds it open, so urine can travel from the bladder back up the ureter. This is known as *reflux*. The effect of reflux of urine up to the kidney may be detrimental.

The Study Group was asked to address the following questions:

1. Can the stent design be improved to minimise encrustation of the top curl?
2. Does the stent cause reflux, and if so how much?
3. Can the stented PUJ and ureter be modelled with respect to the flow?
4. What are the effects of the holes, and would more or fewer be advantageous?

4.2 Encrustation

After the stent is inserted, a bacterial *biofilm* is quickly deposited on its surface, which provides nucleation sites for crystalline deposits of salts in solution in the urine, predominantly calcium oxylate and calcium phosphate. Over several months the stent becomes encrusted with these crystals which, as well as causing discomfort, can lead to further blockage and make the removal of the stent problematic. Although stents may be coated with a range of biomaterials aimed at preventing cell-surface interactions, they currently have to be replaced about every 6 months in long-term patients. Since the stents are expensive (around £500 each), and urologists' time is expensive, and the patient would

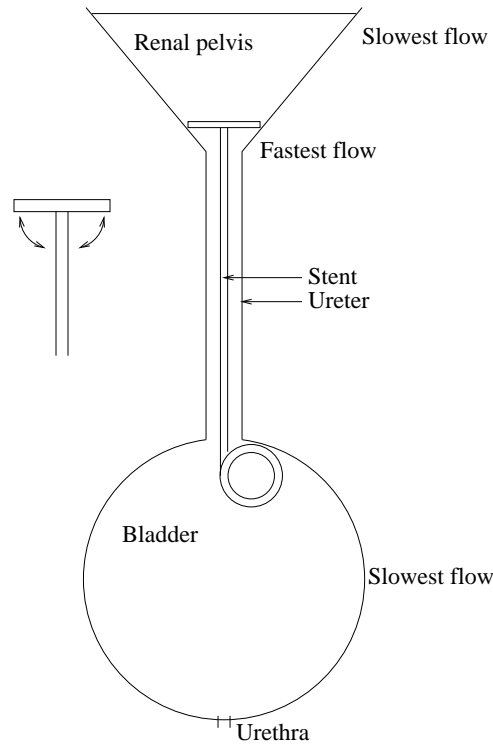


Figure 3: Schematic showing modified design, which impinges less on the “stagnant zones” (where flow is slowest).

prefer to keep stent insertions to a minimum as the process can be very uncomfortable, it is desirable on all counts to maximise the time for which a stent can be left in place.

Almost all of the encrustation observed occurs either on the extreme curled portion of the stent in the renal pelvis, or, to a lesser extent, on the extreme curled portion of the stent in the bladder. A crude model of the renal pelvis-ureter-bladder system is to imagine a rubber tube connecting a funnel (the renal pelvis) and a balloon (the ureter; see figure 2). It is clear from elementary fluid dynamics that the flow of urine is most sluggish at the widest parts of the funnel and the balloon, while it will be fastest in the ureter, including at its entry and exit. Currently the stent design is such that the circular curl at the upper end has more or less the same radius as the renal pelvis cavity. Since the whole system is always full of urine (no air can enter) this means that the top portion of the stent is always situated in more-or-less stagnant urine, providing ideal conditions for the build-up of crystals on the surface. The situation is similar at the bladder end. It seems likely that if the stent design can be changed so that the stent does not sit in these stagnant regions but in the faster flow near the entry and exit of the ureter, the encrustation should be significantly less.

With this in mind, it was suggested that the design of the upper end (the renal pelvis end) could be changed to a T-shape, with sprung arms which will lie parallel to the stent tube during insertion, but which spring out again when the renal pelvis is reached, anchoring the stent at that end. This design should mean that the stent occupies considerably less of the renal pelvis and remains close to the ureter entrance.

At the lower end the design is more problematic, as the bladder is very easily irritated and the T-design may well cause considerable discomfort. The stent must still be

anchored there, otherwise it will disappear up the ureter. Suggested options to minimise encrustation here include using the current design but with a tighter curl, to keep it in a faster flow region, or flaring the end like a trumpet, to make it wider than the constriction at the VUJ. However, encrustation at the bladder end is less of an issue than it is at the renal pelvis end, and even modifying the design at the upper end only should mean that stents need changing less regularly.

With regard to the reflux issue however, we note that there is an available design which has only one J-end (the renal pelvis end), the lower J being replaced by a fine strong nylon loop attached to a fine 3cm polyethylene tube anchor to prevent upward migration of the stent [1]. Since the lower end is only a thread, the VUJ is able to close around it when urinating, or during a bladder twitch, preventing reflux.

4.3 Preliminary considerations

Physiological parameter values and definitions

In order to begin to address the question of how the stent might facilitate reflux of urine, we consider here some simple models. We start by listing the dimensional governing parameters of the system, with estimations of their physiological values. We use a star to denote dimensional quantities, since we shall nondimensionalise later and work with dimensionless quantities.

μ^* = viscosity of urine, which we assume to be the same as that of water, namely $0.654 \text{ g cm}^{-1} \text{ sec}^{-1} = 0.0654 \text{ kg m}^{-1} \text{ sec}^{-1}$ at 40° C .

P_b^* = pressure in the bladder. This is usually 2-5 cm H_2O , but during a twinge reaches 30 cm H_2O , and on voiding the bladder can reach 50 cm H_2O . We may regard it as a specified function of time, providing a boundary condition on the pressure.

P_k^* = pressure in the renal pelvis; around 20 cm H_2O in stented patients. Since the PUJ lies about 20 cm above the bladder, the dominant cause of the pressure difference is hydrostatic due to gravity. Thus when lying down, the PUJ and bladder are at essentially the same pressure. Again we regard this as specified function of time in the model.

L^* = total length of ureter, approximately 25cm.

a^* = radius of stent, approximately 1mm

b^* = radius of ureter, usually less than 3mm.

h^* = thickness of stent wall, approximately 0.5mm.

ρ^* = density of urine, again assumed to be that of water, namely $1 \text{ g cm}^{-3} = 10^3 \text{ kg m}^{-3}$.

Throughout this report we make the simplifying assumption that the stent-ureter system is axisymmetric. The stent will be modelled (in §4.4) as a rigid tube with a porous membrane, and the ureter as a collapsible tube. The basic geometry is sketched in figure 4. We use cylindrical polar coordinates, with the z -axis lying along the centre of the stent (and ureter), in which the velocity of the fluid (urine) is represented by

$$\mathbf{u}^* = u^*(r^*, z^*, t^*)\mathbf{e}_z + v^*(r^*, z^*, t^*)\mathbf{e}_r. \quad (4.1)$$

Gravity (represented by g^*) is assumed to act along the z -direction.¹ The pressures in

¹Even if it has a component perpendicular to this direction its effect will not enter the leading order equations in the r - and θ -equations, so it is simplest to assume this at the outset. If the patient is lying down, the gravity parameter can be set to zero in the model.

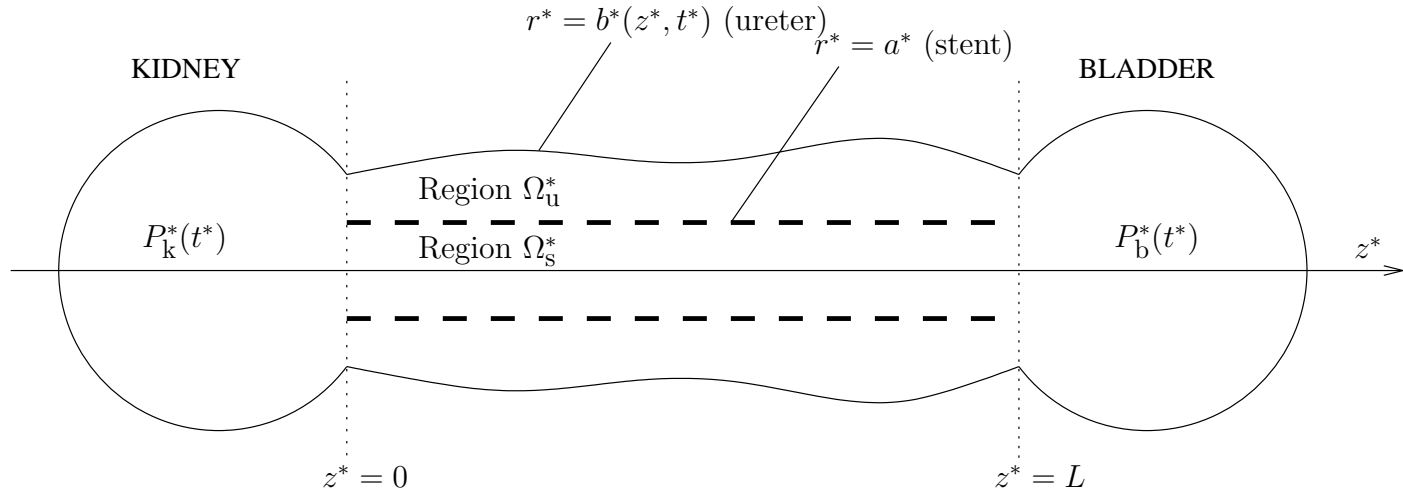


Figure 4: Schematic showing coordinate system and definitions used.

the stent interior (region Ω_s^*) and in the gap between the stent and the ureter wall (region Ω_u^*) will be denoted by p_s^* and p_u^* , respectively (we make use of the ‘s’ and ‘u’ elsewhere to distinguish between other quantities such as velocity in these two regions). We shall use the small aspect ratio of the system a^*/L^* , $b^*/L^* \ll 1$ to construct asymptotic reductions of the governing equations.

Timescales for reflux

In the following we make some simple order of magnitude estimates for the timescales on which urine can flow back up the ureter when the pressure in the bladder exceeds that in the renal pelvis. We consider two idealised scenarios: a non-porous stent (like a drinking-straw in the ureter); and an extremely porous stent (like a fine wire mesh that acts to hold the ureter open, but allows flow freely through its sides).

(i) Non-porous stent

In a non-porous stent, the flow from the bladder to the PUJ can only be via the interior of the stent. Since the stent is long and thin, this flow will be assumed to have a Poiseuille form, which for a cylindrically symmetric tube gives velocity:

$$|u^*| = \frac{1}{4\mu^*L^*}(P_b^* - P_k^*)(a^{*2} - r^{*2}). \quad (4.2)$$

We assume here that $P_b^* > P_k^*$, otherwise reflux will not occur with this simple model. Thus the dimensional flow rate Q^* satisfies

$$|Q^*| = 2\pi \int_0^{a^*} u^* r^* dr^* = \frac{\pi(P_b^* - P_k^*)a^{*4}}{8\mu^*L^*}. \quad (4.3)$$

The mean value of $|u^*|$ (averaged over the cross-section) is given by the flux divided by the area:

$$\langle |u^*| \rangle = \frac{|Q^*|}{\pi a^{*2}} = \frac{(P_b^* - P_k^*)a^{*2}}{8\mu^*L^*}. \quad (4.4)$$

Thus we can estimate the timescale for reflux, T^* , as

$$T^* = \frac{L^*}{\langle |u^*| \rangle} = \frac{8\mu^* L^{*2}}{(P_b^* - P_k^*) a^{*2}} \approx \begin{cases} 32.7 \text{ s} & \text{during a twinge} \\ 10.9 \text{ s} & \text{during voiding,} \end{cases} \quad (4.5)$$

using the estimates provided above ($(P_b^* - P_k^*)$ is taken to be 10cm H₂O or 1000 Pa during a twinge, and 30cm H₂O or 3000 Pa during voiding).

(ii) Extremely porous stent

In this case we assume that the stent simply acts to hold the ureter open at the blockage, allowing urine to flow, and we take this flow to have a Poiseuille form for a tube of varying radius $b^*(z^*)$, that is

$$|u^*| = \frac{1}{4\mu^*} (b^*(z^*)^2 - r^{*2}) \left| \frac{\partial p^*}{\partial z^*} \right|, \quad (4.6)$$

where $p^*(z^*)$ is the pressure at height z^* in the tube. Integrating across the tube we find the total flux down the tube satisfies

$$|Q^*| = \int_0^{b^*} 2\pi r^* |u^*| dr^* = \frac{\pi b^*(z^*)^4}{8\mu^*} \left| \frac{\partial p^*}{\partial z^*} \right|. \quad (4.7)$$

To maintain generality, we assume that $\partial p^*/\partial z^*$ is genuinely dependent on z^* but that Q^* is not, thus we have

$$\left| \frac{\partial p^*}{\partial z^*} \right| = \frac{8\mu^* |Q^*|}{\pi b^*(z^*)^4},$$

which (on integrating) gives the pressure at any given point of the ureter. Integrating between $z^* = 0$ and $z^* = L^*$ gives an expression for the total pressure drop:

$$P_b^* - P_k^* = \frac{8\mu^* |Q^*|}{\pi} \int_0^{L^*} \frac{d\tilde{z}^*}{b^*(\tilde{z}^*)^4}. \quad (4.8)$$

The average flow rate in the ureter is given by $\langle |u^*| \rangle = |Q^*|/(\pi b^*(z^*)^2)$, as in (i) above. Rearranging (4.8), we find

$$|Q^*| = \frac{\pi(P_b^* - P_k^*)}{8\mu^* \int_0^{L^*} b^*(\tilde{z}^*)^{-4} d\tilde{z}^*},$$

thus

$$\frac{1}{\langle |u^*| \rangle} = \frac{\pi b^*(z^*)^2}{|Q^*|} = \frac{8\mu^* b^*(z^*)^2}{(P_b^* - P_k^*)} \int_0^{L^*} \frac{d\tilde{z}^*}{b^*(\tilde{z}^*)^4}.$$

Now we use the relationship $d|z^*|/dt^* = \langle |u^*| \rangle$ for fluid flowing in the ureter. Since u^* is independent of t^* we can separate variables and integrate over $0 \leq z^* \leq L^*$ to find the time T^* taken for fluid to travel the length of the ureter:

$$T^* = \left| \int_0^{L^*} \frac{dz^*}{\langle |u^*| \rangle} \right| = \frac{8\mu^*}{(P_b^* - P_k^*)} \int_0^{L^*} b^*(z^*)^2 dz^* \int_0^{L^*} \frac{1}{b^*(z^*)^4} dz^* \approx \begin{cases} 3.6 \text{ s} & \text{during a twinge} \\ 1.2 \text{ s} & \text{during voiding,} \end{cases}$$

with the same estimates for $(P_b^* - P_k^*)$ as used in (i) above. These estimates suggest that we do not expect urine to reflux all the way back to the kidney during a bladder twinge, but that this may well occur during voiding of the bladder, which can last for some time.

(Note that in both cases (i) and (ii) it is also possible to estimate how far the fluid has refluxed back along the ureter in a given time.)

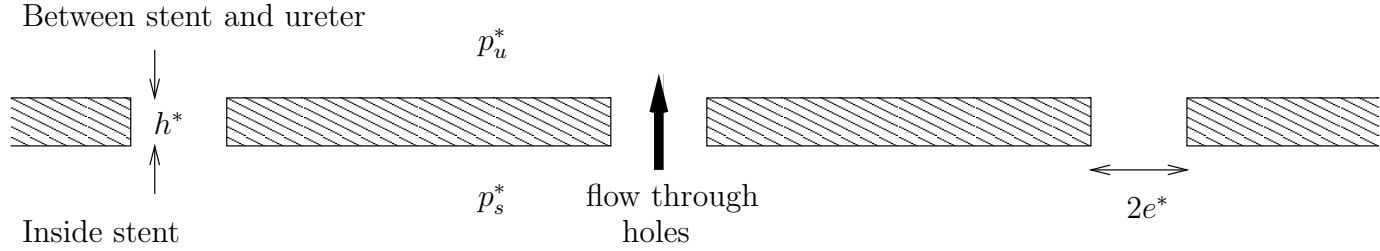


Figure 5: Flow through the porous wall of the stent.

Flow through the porous stent wall

Since the stent has holes in its sides, urine will flow between stent and ureter if there is a pressure differential across the stent wall. The flux per unit area from stent to ureter, Q_{su}^* say, can be evaluated in terms of the stent parameters. A close-up of the stent wall is indicated in figure 5, showing the pores through which the fluid flows, and their dimensions. Considering an individual pore, the flow through it will be approximately Poiseuille, with $v^* = (p_s^* - p_u^*)(e^{*2} - \tilde{r}^{*2})/(4\mu^*h^*)$, where \tilde{r}^* is the radial distance from the centre of the pore, e^* is the pore radius, h^* is the thickness of the stent wall, and p_s^* and p_u^* are the pressures inside the stent and in the gap between stent and ureter, respectively. The flux through this single hole (hence we use a '1' superscript) is thus

$$q_{\text{su}}^{*(1)} = \iint_{\text{pore}} v^* dS = \frac{\pi(p_s^* - p_u^*)e^{*4}}{8\mu^*h^*},$$

hence the total flux per unit area of stent surface is

$$Q_{\text{su}}^* = \frac{\pi(p_s^* - p_u^*)e^{*4}n^*}{8\mu^*h^*},$$

where n^* is the number of pores per unit area of surface. For the purpose of our calculations it is much simpler to treat the tube as being uniformly porous, in which case this flux per unit area may be interpreted as a radial velocity through the stent wall. Hence, assuming that the stent wall thickness h^* is much smaller than the stent radius, this gives a condition on the radial velocity v^* to apply at the stent wall $r^* = a^*$:

$$v_{\text{u}}^* = \lambda^*(p_s^* - p_u^*) = v_s^*, \quad \lambda^* = \frac{\pi e^{*4}n^*}{8\mu^*h^*}. \quad (4.9)$$

4.4 Collapsible tube model of ureter

We again refer to figure 4 for the basic geometry. We model the situation in which the stent is taken to be a rigid porous tube, and the ureter is an elastic membrane which will stretch if there is a pressure differential across it. The ambient pressure in the body outside the ureter p_{body}^* is taken to be hydrostatic, induced only by gravity.

The flow is governed by the Navier-Stokes equations for this velocity field with a pressure $p^*(r^*, z^*, t^*)$, subject to the following boundary conditions on the ureter and stent walls:

$$u_{\text{u}}^* = 0, \quad v_{\text{u}}^* = \frac{\partial b^*}{\partial t^*}, \quad p_{\text{u}}^* - p_{\text{body}}^* = k^*(z^*)(b^*(z^*, t^*) - b_{\text{a}}^*(z^*)), \quad \text{on } r^* = b^*(z^*, t^*) \quad (4.10)$$

where $b_a^*(z^*)$ denotes the ‘ambient’ state of the ureter, when the pressure within it is also p_{body}^* . If we assume that the ureter is sufficiently elastic that it contracts about the stent in this situation, we may take $b_a^*(z^*) \equiv a^*$ to obtain an approximate wall law. Implicit in this law is the assumption that $b^*(z^*, t^*)$ can never be less than a^* , hence this condition applies only to a stented ureter—an unstented ureter could, in principle, collapse in on itself if the internal pressure is low enough. The function $k^*(z^*)$ is a measure of how difficult it is to stretch the ureter: if $k^*(z^*)$ is very large at some point z^* then a very large internal pressure is required to stretch the ureter. This enables us to model a blocked ureter. At the porous stent wall we have the boundary condition (4.9) derived earlier, giving the fluid flow between stent and ureter:

$$v_s^* = \lambda^*(p_s^* - p_u^*) = v_u^* \quad \text{on } r^* = a^*; \quad \lambda^* = \frac{\pi e^{*4} n^*}{8\mu^* h^*}. \quad (4.11)$$

We assume a no-slip condition on the z^* -component of velocity on either side of the wall:

$$u_s^* = 0 = u_u^* \quad \text{on } r^* = a^*. \quad (4.12)$$

We nondimensionalise the Navier-Stokes equations as usual, scaling z^* with L^* , r^* with the stent radius $a^* = \epsilon L^*$ ($0 < \epsilon \ll 1$), pressure with Π^* (to be determined), velocity component u^* with $U^* = \Pi^* a^{*2} / (\mu^* L^*)$ (to give a leading-order balance in the z -component of the Navier-Stokes equations), and v^* with $V^* = \epsilon U^*$ (to give a balance in the continuity equation). Time is scaled with L^*/U^* . We write $B(z, t) = b^*(L^*z, L^*t/U^*) / (\epsilon L^*)$ as the dimensionless ureter radius; the dimensionless stent radius is obviously 1.

With these scalings, to leading order in ϵ the dimensionless Navier-Stokes equations yield

$$\frac{\partial p}{\partial z} = \frac{1}{r} \frac{\partial}{\partial r} \left(r \frac{\partial u}{\partial r} \right) + \text{Bo}, \quad (4.13)$$

$$\frac{\partial p}{\partial r} = 0 \quad \Rightarrow \quad p = p(z, t), \quad (4.14)$$

$$\frac{1}{r} \frac{\partial}{\partial r} (rv) + \frac{\partial u}{\partial z} = 0, \quad (4.15)$$

where $\text{Bo} = \rho^* g^* L^* / \Pi^*$ is the Bond number. The ambient pressure outside the ureter is then given by $p_{\text{body}} = z\text{Bo}$, taking $p_{\text{body}} = 0$ when $z = 0$ without loss of generality. The boundary conditions at the ureter wall become:

$$u_u = 0, \quad v_u = \frac{\partial B}{\partial t}, \quad p_u - z\text{Bo} = K(z)(B(z, t) - 1) \quad \text{on } r = B(z, t), \quad (4.16)$$

where $K(z) = \epsilon L^* k^*(L^*z) / \Pi^*$ is the dimensionless ureter stiffness. In fact, since p_u is independent of r , (4.16) gives the pressure throughout Ω_u . At $z = 0, 1$ we have dimensionless pressures $p = P_k(t)$, $p = P_b(t)$ respectively.

At the stent wall we have

$$u_u = 0 = u_s, \quad v_u = \frac{\Lambda}{16} (p_s - p_u) = v_s \quad \text{on } r = 1, \quad (4.17)$$

where $\Lambda = 2\pi e^{*4} n^* / (h^* L^* \epsilon^3)$ is the dimensionless stent porosity. It is a rough measure of how much fluid will flow out through the stent pores, compared with the fluid that goes

directly down through the stent: if Λ is large then it is easier for fluid under pressure to escape through the pores, rather than being pushed all the way along the tube.

Obviously parameters vary from one stent to another of different manufacture, but a ‘typical’ JJ-stent has circumference 6mm (hence radius $a^* = 0.955\text{mm}$), length $L^* = 250\text{mm}$ and wall thickness $h^* \approx 0.5\text{mm}$, with holes (of radius $e^* \approx 0.25\text{mm}$) punched about every 10mm along its length in two loose spirals. Thus the total number of holes in the stent is around 50, and its surface area is $6 \times 250\text{mm}^2$, giving $n^* = (1/60)\text{mm}^{-2}$. The stent aspect ratio $\epsilon = 0.955/250 = 0.00382$. These numbers give a value for Λ of

$$\Lambda \approx 117.4; \quad (4.18)$$

however it is a trivial matter to change this number significantly by introducing very minor changes in the stent design, and we may regard this as an adjustable parameter.

Working with the reduced pressure $\hat{p} = p - z\text{Bo}$ we can solve for u using (4.13) and the no-slip conditions:

$$u_s = \frac{1}{4} \frac{\partial \hat{p}_s}{\partial z} (r^2 - 1), \quad u_u = \frac{1}{4} \frac{\partial \hat{p}_u}{\partial z} (r^2 - 1 + C_1 \log r^2), \quad (4.19)$$

where

$$C_1 = -\frac{B^2 - 1}{\log B^2}. \quad (4.20)$$

The radial velocity v is then given by (4.15) as

$$v_s = \frac{1}{16} \frac{\partial^2 \hat{p}_s}{\partial z^2} r(2 - r^2), \quad (4.21)$$

$$v_u = -\frac{1}{16} \frac{\partial^2 \hat{p}_u}{\partial z^2} r(r^2 - 2 + 2C_1(\log r^2 - 1)) - \frac{1}{8} \frac{\partial \hat{p}_u}{\partial z} \frac{\partial C_1}{\partial z} r(\log r^2 - 1) - \frac{f(z, t)}{16r},$$

where $f(z, t)$ is to be determined by the conditions (4.16) and (4.17). The pressure \hat{p}_u is given by (4.16) as

$$\hat{p}_u = K(z)(B(z, t) - 1), \quad (4.22)$$

and using conditions (4.17) in (4.21), \hat{p}_s satisfies:

$$\frac{\partial^2 \hat{p}_s}{\partial z^2} = \Lambda(\hat{p}_s - \hat{p}_u) \quad \Rightarrow \quad \hat{p}_u = \hat{p}_s - \frac{1}{\Lambda} \frac{\partial^2 \hat{p}_s}{\partial z^2}. \quad (4.23)$$

On $r = B(z, t)$ (4.16) gives

$$\begin{aligned} -16B \frac{\partial B}{\partial t} &= \frac{\partial^2 \hat{p}_u}{\partial z^2} B^2 (B^2 - 2 + 2C_1(\log B^2 - 1)) + 2 \frac{\partial \hat{p}_u}{\partial z} \frac{\partial C_1}{\partial z} B^2 (\log B^2 - 1) + f(z, t) \\ &= \frac{\partial^2 \hat{p}_u}{\partial z^2} B^2 (B^2 - 2) + 2B^2 (\log B^2 - 1) \frac{\partial}{\partial z} \left(C_1 \frac{\partial \hat{p}_u}{\partial z} \right) + f(z, t), \end{aligned}$$

while on $r = 1$ (4.17) gives (after a little rearrangement)

$$-\Lambda(\hat{p}_s - \hat{p}_u) = -\frac{\partial^2 \hat{p}_u}{\partial z^2} - 2 \frac{\partial}{\partial z} \left(C_1 \frac{\partial \hat{p}_u}{\partial z} \right) + f(z, t).$$

Eliminating $f(z, t)$ between these two equations gives a single equation linking $B(z, t)$, \widehat{p}_s and \widehat{p}_u (C_1 defined in (4.20) depends only on $B(z, t)$), which (using (4.23)) may be written in the form

$$8\frac{\partial\beta}{\partial t} + \frac{\partial^2\widehat{p}_u}{\partial z^2}\beta(\beta-2) + \frac{\partial^2\widehat{p}_u}{\partial z^2} - \frac{\partial^2\widehat{p}_s}{\partial z^2} - 2\frac{\partial}{\partial z} \left(\frac{\partial\widehat{p}_u}{\partial z} \frac{(\beta-1)}{\log\beta} \right) (\beta\log\beta - \beta + 1) = 0 \quad (4.24)$$

where $\beta = B^2$.

Equation (4.22) gives $B(z, t)$ in terms of \widehat{p}_u and hence, using (4.23), in terms of \widehat{p}_s :

$$B(z, t) = 1 + \frac{1}{K(z)} \left(\widehat{p}_s - \frac{1}{\Lambda} \frac{\partial^2\widehat{p}_s}{\partial z^2} \right).$$

Hence substituting in (4.24) for \widehat{p}_u and B (or β) in terms of \widehat{p}_s , using the above, we can obtain a single 4th-order nonlinear partial differential equation for the reduced pressure in the stent, \widehat{p}_s . Clearly, each of \widehat{p}_s and \widehat{p}_u will be equal to $P_k(t)$ at $z = 0$, and equal to $(P_b(t) - \text{Bo})$ at $z = 1$. Thus we have boundary values for \widehat{p}_s and, using (4.23), for $\partial^2\widehat{p}_s/\partial z^2$ at $z = 0, 1$:

$$\begin{aligned} \widehat{p}_s &= P_k(t) \equiv \widehat{P}_k(t), & \frac{\partial^2\widehat{p}_s}{\partial z^2} &= 0, & \text{at } z &= 0, \\ \widehat{p}_s &= P_b(t) - \text{Bo} \equiv \widehat{P}_b(t), & \frac{\partial^2\widehat{p}_s}{\partial z^2} &= 0, & \text{at } z &= 1, \end{aligned} \quad (4.25)$$

An initial condition completes the system. If $\widehat{p}_s(z, 0)$ is specified this is straightforward, but if *e.g.* the initial ureter shape $B(z, 0)$ is specified then we have to solve an ordinary differential equation

$$\frac{\partial^2\widehat{p}_s}{\partial z^2} - \Lambda\widehat{p}_s = -\Lambda K(z)(B(z, 0) - 1)$$

to determine $\widehat{p}_s(z, 0)$. This 4th order PDE will be very complicated in general, and we now consider simplifications.

Large porosity limit $\Lambda \gg 1$

Given the estimate (4.18) of Λ for a ‘typical’ stent, we write $\varepsilon_1 = 1/\Lambda$ and write the functions \widehat{p}_u , \widehat{p}_s and B (or β) as asymptotic expansions in powers of ε_1 ($0 < \varepsilon_1 \ll 1$):

$$\begin{aligned} \widehat{p}_u &= \widehat{p}_{u0} + \varepsilon_1\widehat{p}_{u1} + \dots, \\ \widehat{p}_s &= \widehat{p}_{s0} + \varepsilon_1\widehat{p}_{s1} + \dots, \\ B &= B_0 + \varepsilon_1 B_1 + \dots, \\ \beta &= \beta_0 + \varepsilon_1\beta_1 + \dots \equiv B_0^2 + 2\varepsilon_1 B_0 B_1 + \dots. \end{aligned} \quad (4.26)$$

Substituting the asymptotic expansions (4.26) in (4.23) and (4.22), leading order gives

$$\widehat{p}_{s0} = \widehat{p}_{u0} = K(z)(B_0(z, t) - 1). \quad (4.27)$$

Using this in (4.24) gives a second order nonlinear PDE for $\beta_0(z, t) = B_0^2(z, t)$:

$$8\frac{\partial\beta_0}{\partial t} + \beta_0(\beta_0 - 2)\frac{\partial^2}{\partial z^2} [K(z)(B_0 - 1)] - 2(\beta_0\log\beta_0 - \beta_0 + 1)\frac{\partial}{\partial z} \left(\frac{(\beta_0 - 1)}{\log\beta_0} \frac{\partial}{\partial z} [K(z)(B_0 - 1)] \right) = 0 \quad (4.28)$$

The boundary conditions on B_0 come from the pressure conditions at $z = 0, 1$ via (4.27):

$$B_0(0, t) = 1 + \frac{\widehat{P}_k(t)}{K(0)}, \quad B_0(1, t) = 1 + \frac{\widehat{P}_b(t)}{K(1)}, \quad (4.29)$$

and we must also specify the initial ureter shape $B(z, 0)$.

Further simplifications

There are various further asymptotic simplifications we can make to the above model. The first possibility we consider is a perturbation about the steady solution to the above model,

$$\widehat{p}_{u0} = 1 = \widehat{p}_{s0}, \quad B_0(z) = 1 + \frac{1}{K(z)},$$

for arbitrary elasticity function $K(z)$. We know, from the Introduction, that the pressure in the renal pelvis is about 20cm H₂O in a stented patient. With our choice of $z = 0$ for zero hydrostatic pressure, this is also the reduced pressure \widehat{P}_k^* in the renal pelvis. The bladder pressure is normally 2-3cm H₂O, but during voiding reaches 50cm H₂O, giving a reduced (dimensional) voiding pressure in an upright patient of $\widehat{P}_b^* = (50 - 25)$ cm H₂O (25cm being the length of the ureter in the z -direction). Hence during voiding at least (which can easily last long enough for a nearly steady state to be set up) the reduced pressures at either end of the ureter are nearly equal. If the pressure is made dimensionless with a typical value of the pressure in the renal pelvis, then these dimensional reduced pressures at the ends are both close to 1.

We write

$$\left. \begin{aligned} B_0(z, t) &= (1 + 1/K(z)) + \delta B_{01}(z, t) + O(\delta^2), \\ \beta_0(z, t) &= (1 + 1/K(z))^2 + \delta \beta_{01}(z, t) + O(\delta^2) \\ &\equiv (1 + 1/K(z))^2 + 2\delta(1 + 1/K(z))B_{01}(z, t) + O(\delta^2), \\ \widehat{p}_{u0}(z, t) &= 1 + \delta \widehat{p}_{u01} + O(\delta^2), \\ \widehat{p}_{s0}(z, t) &= 1 + \delta \widehat{p}_{s01} + O(\delta^2), \\ \widehat{P}_k(t) &= 1 + \delta \widehat{P}_{k1}(t) + O(\delta^2) \quad \widehat{P}_b(t) = 1 + \delta \widehat{P}_{b1}(t) + O(\delta^2) \end{aligned} \right\} 0 < \varepsilon_1 \ll \delta \ll 1 \quad (4.30)$$

($\widehat{P}_{k1}(t)$ and $\widehat{P}_{b1}(t)$ are specified). We substitute these expansions into (4.28) above. Order 1 terms vanish automatically, and at order δ we obtain the equation:

$$\begin{aligned} 16B_{00} \frac{\partial B_{01}}{\partial t} &= \left(B_{00}^4 - \frac{2(B_{00}^2 - 1)^2}{\log B_{00}^2} \right) \frac{\partial^2}{\partial z^2} (KB_{01}) + \\ &2(B_{00}^2 \log B_{00}^2 - B_{00}^2 + 1) \frac{\partial}{\partial z} \left(\frac{B_{00}^2 - 1}{\log B_{00}^2} \right) \frac{\partial}{\partial z} (KB_{01}) = 0, \end{aligned} \quad (4.31)$$

where $B_{00}(z) = 1 + 1/K(z)$. Clearly this is much simplified if $K(z)$ is just a constant (which should be a good approximation for an unobstructed ureter), since then we get a diffusion equation

$$\frac{\partial B_{01}}{\partial t} = D \frac{\partial^2 B_{01}}{\partial z^2} \quad D = \frac{K}{16B_{00}} \left[B_{00}^4 - \frac{2(B_{00}^2 - 1)^2}{\log B_{00}^2} \right] \quad (4.32)$$

(D is always positive for $K > 0$, but tends to infinity as $B_{00} \rightarrow 1^+$, that is, as $K \rightarrow \infty$: $D \sim 1/(16(B_{00} - 1))$). This equation has similarity solutions of the form: $B_{01}(z, t) = (t + t_0)^\alpha F((z + z_0)/(2\sqrt{D(t + t_0)}))$, for any α , provided F satisfies the ODE

$$F''(\eta) = 4\alpha F(\eta) - 2\eta F'(\eta).$$

The parameters z_0 and t_0 just represent translations in z and t . As is well-known, this equation can be integrated for 2 special values of α .

Case $\alpha = 0$

In this case the general solution is

$$B_{01} = c_1 \operatorname{erf}(\eta) + c_2; \quad \eta = \frac{(z + z_0)}{2\sqrt{D(t + t_0)}}, \quad \operatorname{erf}(x) := \frac{2}{\sqrt{\pi}} \int_0^x e^{-s^2} ds, \quad (4.33)$$

for constants c_1 , c_2 , z_0 and t_0 . The boundary conditions are given by (4.29):

$$B_{01}(0, t) = c_1 \operatorname{erf}\left(\frac{z_0}{2\sqrt{D(t + t_0)}}\right) + c_2 = \frac{\widehat{P}_{k1}(t)}{K}, \quad (4.34)$$

$$B_{01}(1, t) = c_1 \operatorname{erf}\left(\frac{(1 + z_0)}{2\sqrt{D(t + t_0)}}\right) + c_2 = \frac{\widehat{P}_{b1}(t)}{K}. \quad (4.35)$$

Hence such solutions are possible only for boundary conditions of this specific form.

When the $\delta \ll 1$ solution is relevant (nearly-equal kidney and bladder reduced pressures, probably during urination), we can model a further small bladder ‘twinge’ by a solution of this kind, in which the bladder pressure suddenly rises to $1 + \delta$, then decays back to the constant value 1, while the pressure in the renal pelvis remains fixed at 1. Taking $z_0 = 0 = t_0$, the relevant solution has $c_1 = 1/K$, $c_2 = 0$. The bladder pressure required to generate this solution is thus

$$\widehat{P}_b(t) = 1 + \delta \operatorname{erf}\left(\frac{1}{2\sqrt{Dt}}\right) + O(\delta^2). \quad (4.36)$$

The ureter wall is then described by

$$B_0(z, t) = 1 + \frac{1}{K} + \frac{\delta}{K} \operatorname{erf}\left(\frac{z}{2\sqrt{Dt}}\right) + O(\delta^2).$$

Case $\alpha = -1/2$

In this case $B_{10} = F((z + z^*)/(2\sqrt{D(t + t^*))})/\sqrt{t + t^*}$, where

$$F(\eta) = e^{-\eta^2} (c_1 \int_0^\eta e^{s^2} ds + c_2)$$

for constants c_1 and c_2 . The boundary conditions (4.34) and (4.35) on B_{01} at $z = 0, 1$ are applicable, and if we again seek a solution for which there is no excess pressure in the renal pelvis, but a pulse in the bladder pressure at $t = 0$ then we take $z^* = 0 = t^*$, and

$$c_2 = 0, \quad \widehat{P}_{b1}(t) = \frac{Kc_1}{\sqrt{t}} e^{-\frac{1}{4Dt}} \int_0^{\frac{1}{2\sqrt{Dt}}} e^{s^2} ds, \quad (4.37)$$

the value of c_1 being fixed by the size of the initial pulse. The limit as $t \rightarrow 0$ of $\widehat{P}_{b1}(t)$ as given by this expression is $K\sqrt{D}c_1$, so if we want an initial pulse $\widehat{P}_b(0) = 1 + \delta$ as before we choose $c_1 = 1/(K\sqrt{D})$. Hence the solution for the wall shape is:

$$B_0 = 1 + \frac{1}{K} + \delta \frac{e^{-\frac{z^2}{4Dt}}}{K\sqrt{Dt}} \int_0^{\frac{z}{2\sqrt{Dt}}} e^{s^2} ds + O(\delta^2). \quad (4.38)$$

Solutions with periodic forcing

For constant K there are also solutions of (4.32) driven by periodic forcing from the kidney pressure. If the time dependence of this forcing is of the form $\exp(i\omega t)$ (so ω is the dimensionless period of the forcing) then these solutions have the general form

$$\begin{aligned} B_{01}(z, t) = & c_1 \exp\left(z\sqrt{\frac{\omega}{2D}}\right) \left(\cos \omega t \sin\left(z\sqrt{\frac{\omega}{2D}}\right) + \sin \omega t \cos\left(z\sqrt{\frac{\omega}{2D}}\right)\right) + \\ & c_2 \exp\left(-z\sqrt{\frac{\omega}{2D}}\right) \left(\cos \omega t \sin\left(z\sqrt{\frac{\omega}{2D}}\right) - \sin \omega t \cos\left(z\sqrt{\frac{\omega}{2D}}\right)\right) + \\ & c_3 \exp\left(z\sqrt{\frac{\omega}{2D}}\right) \left(\cos \omega t \cos\left(z\sqrt{\frac{\omega}{2D}}\right) - \sin \omega t \sin\left(z\sqrt{\frac{\omega}{2D}}\right)\right) + \\ & c_4 \exp\left(-z\sqrt{\frac{\omega}{2D}}\right) \left(\cos \omega t \cos\left(z\sqrt{\frac{\omega}{2D}}\right) + \sin \omega t \sin\left(z\sqrt{\frac{\omega}{2D}}\right)\right). \end{aligned} \quad (4.39)$$

If we assume that the kidney exerts a pulsing pressure $1 + \delta\widehat{\mathcal{P}}_{k1} \cos \omega t$ at $z = 0$, and that the bladder pressure is maintained constant at $z = 1$, then by (4.29) this translates into boundary conditions on $B_{01}(z, t)$:

$$B_{01}(0, t) = \frac{\widehat{\mathcal{P}}_{k1}}{K} \cos \omega t, \quad B_{01}(1, t) = 0. \quad (4.40)$$

The solution to the problem with these boundary conditions is:

$$\begin{aligned} B_{01} = & c_1 \cos \omega t \sin\left((z-1)\sqrt{\frac{\omega}{2D}}\right) \cosh\left((z-1)\sqrt{\frac{\omega}{2D}}\right) + \\ & c_1 \sin \omega t \cos\left((z-1)\sqrt{\frac{\omega}{2D}}\right) \sinh\left((z-1)\sqrt{\frac{\omega}{2D}}\right) + \\ & c_3 \cos \omega t \cos\left((z-1)\sqrt{\frac{\omega}{2D}}\right) \sinh\left((z-1)\sqrt{\frac{\omega}{2D}}\right) - \\ & c_3 \sin \omega t \sin\left((z-1)\sqrt{\frac{\omega}{2D}}\right) \cosh\left((z-1)\sqrt{\frac{\omega}{2D}}\right), \end{aligned} \quad (4.41)$$

where

$$c_1 = -\frac{\widehat{\mathcal{P}}_{k1}}{K} \frac{\cosh \sqrt{\frac{\omega}{2D}} \sin \sqrt{\frac{\omega}{2D}}}{\cosh^2 \sqrt{\frac{\omega}{2D}} - \cos^2 \sqrt{\frac{\omega}{2D}}}, \quad c_3 = -\frac{\widehat{\mathcal{P}}_{k1}}{K} \frac{\sinh \sqrt{\frac{\omega}{2D}} \cos \sqrt{\frac{\omega}{2D}}}{\cosh^2 \sqrt{\frac{\omega}{2D}} - \cos^2 \sqrt{\frac{\omega}{2D}}}. \quad (4.42)$$

We can also consider the case where the reduced pressure in the renal pelvis remains constant, while the bladder undergoes small periodic contractions during urination, leading

to periodic pressure fluctuations $\delta\widehat{\mathcal{P}}_{b1} \cos \omega t$. In this case boundary conditions (4.40) are replaced by

$$B_{01}(0, t) = 0, \quad B_{01}(1, t) = \frac{\widehat{\mathcal{P}}_{b1}}{K} \cos \omega t, \quad (4.43)$$

and the corresponding solution is

$$B_{01} = c_1 \cos \omega t \sin \left(z \sqrt{\frac{\omega}{2D}} \right) \cosh \left(z \sqrt{\frac{\omega}{2D}} \right) + c_1 \sin \omega t \cos \left(z \sqrt{\frac{\omega}{2D}} \right) \sinh \left(z \sqrt{\frac{\omega}{2D}} \right) + c_3 \cos \omega t \cos \left(z \sqrt{\frac{\omega}{2D}} \right) \sinh \left(z \sqrt{\frac{\omega}{2D}} \right) - c_3 \sin \omega t \sin \left(z \sqrt{\frac{\omega}{2D}} \right) \cosh \left(z \sqrt{\frac{\omega}{2D}} \right) \quad (4.44)$$

where

$$c_1 = \frac{\widehat{\mathcal{P}}_{b1}}{K} \frac{\cosh \sqrt{\frac{\omega}{2D}} \sin \sqrt{\frac{\omega}{2D}}}{\cosh^2 \sqrt{\frac{\omega}{2D}} - \cos^2 \sqrt{\frac{\omega}{2D}}}, \quad c_3 = \frac{\widehat{\mathcal{P}}_{b1}}{K} \frac{\sinh \sqrt{\frac{\omega}{2D}} \cos \sqrt{\frac{\omega}{2D}}}{\cosh^2 \sqrt{\frac{\omega}{2D}} - \cos^2 \sqrt{\frac{\omega}{2D}}}. \quad (4.45)$$

Reflux

For any of the solutions of §4.4 the axial velocity u within the stent/ureter system is found from equations (4.19) as

$$u_s(r, z, t) = \frac{\delta}{4} K \frac{\partial B_{01}}{\partial z} (r^2 - 1) + O(\delta^2) \quad 0 < r < 1 \quad (4.46)$$

$$u_u(r, z, t) = \frac{\delta}{4} K \frac{\partial B_{01}}{\partial z} (r^2 - 1 - \frac{B_{00}^2 - 1}{\log B_{00}^2} \log r^2) + O(\delta^2) \quad 1 < r < B_{00} \equiv 1 + 1/K \quad (4.47)$$

From these we can work out the flux of urine $Q(1, t)$ through the bladder entrance $z = 1$:

$$Q_s(1, t) = \int_0^{2\pi} \int_0^1 u_s|_{z=1} r \, dr \, d\theta = -\frac{\pi \delta K}{8} \frac{\partial B_{01}}{\partial z} \Big|_{z=1}, \quad (4.48)$$

$$Q_u(1, t) = \int_0^{2\pi} \int_1^{B_{00}} u_u|_{z=1} r \, dr \, d\theta = -\frac{\pi \delta K}{8} \left(B_{00}^4 - 1 - \frac{2(B_{00}^2 - 1)^2}{\log B_{00}^2} \right) \frac{\partial B_{01}}{\partial z} \Big|_{z=1} \quad (4.49)$$

Hence the total flux $Q(1, t) = Q_s(1, t) + Q_u(1, t)$ is given by

$$Q(1, t) = -2\delta\pi B_{00} D \frac{\partial B_{01}}{\partial z} \Big|_{z=1} \quad (4.50)$$

with D as defined in (4.32).

For the $\alpha = 0$ similarity solution,

$$\frac{\partial B_{01}}{\partial z} \Big|_{z=1} = \frac{e^{-\frac{1}{4Dt}}}{K \sqrt{\pi Dt}}, \quad (4.51)$$

while for the $\alpha = -1/2$ solution

$$\frac{\partial B_{01}}{\partial z} \Big|_{z=1} = \frac{1}{2KDt} \left(1 - \frac{e^{-\frac{1}{4Dt}}}{\sqrt{Dt}} \int_0^{\frac{1}{2\sqrt{Dt}}} e^{s^2} ds \right) = \frac{1}{2KDt} \left(1 - \int_0^{\frac{1}{4Dt}} \frac{e^{-x} dx}{\sqrt{1-4Dtx}} \right) \quad (4.52)$$

The expression on the right-hand side of (4.51) is always positive, increasing from 0 (at $t = 0^+$) to an initial maximum, before decaying like $1/(K\sqrt{\pi Dt})$ as $t \rightarrow \infty$. Hence, since $D > 0$, the net flux at the bladder entrance is negative, and there is persistent reflux in this case.

The behaviour of the expression on the right-hand side of (4.52) is initially negative (a careful asymptotic analysis reveals that it behaves like $-(1 + 6Dt + O(t^2))/K$ as $t \rightarrow 0$), but rapidly becomes positive, decaying for large times like $1/(2KDt)$. Hence although the initial flux of fluid is into the bladder, thereafter there is negative (but decaying) reflux from the bladder back into the ureter.

For the periodic solutions, in the former case (pulsing kidney pressure) we have

$$\left. \frac{\partial B_{01}}{\partial z} \right|_{z=1} = -\sqrt{\frac{\omega}{2D}} \frac{\widehat{\mathcal{P}}_{k1}}{K} \frac{\cosh \sqrt{\frac{\omega}{2D}} \sin \sqrt{\frac{\omega}{2D}} (\cos \omega t + \sin \omega t) + \cos \sqrt{\frac{\omega}{2D}} \sinh \sqrt{\frac{\omega}{2D}} (\cos \omega t - \sin \omega t)}{\cosh^2 \sqrt{\frac{\omega}{2D}} - \cos^2 \sqrt{\frac{\omega}{2D}}},$$

while in the latter case when the bladder pressure is fluctuating,

$$\left. \frac{\partial B_{01}}{\partial z} \right|_{z=1} = \sqrt{\frac{\omega}{2D}} \frac{\widehat{\mathcal{P}}_{b1}}{K} \frac{\cosh \sqrt{\frac{\omega}{2D}} \sinh \sqrt{\frac{\omega}{2D}} (\cos \omega t - \sin \omega t) + \cos \sqrt{\frac{\omega}{2D}} \sin \sqrt{\frac{\omega}{2D}} (\cos \omega t + \sin \omega t)}{\cosh^2 \sqrt{\frac{\omega}{2D}} - \cos^2 \sqrt{\frac{\omega}{2D}}}.$$

For a given value of $B_{00} = 1 + 1/K > 1$ $f(B_{00})$ is a fixed (positive) number, while in either case $\partial B_{01}/\partial z(1, t)$ is periodic in time with period $2\pi/\omega$. Clearly then in these situations too there will be reflux of urine from the bladder back into the ureter, an undesirable occurrence, as outlined in the Introduction.

Stretchy ureter ($|K(z)| \ll 1$)

In this case we write $K(z) = \varepsilon_2 \kappa(z)$ where ε_2 is some small positive quantity, and make asymptotic expansions for functions in powers of ε_2 . From (4.22) and (4.23) however, we then see that either $B(z, t) \gg 1$, or that the pressures \widehat{p}_u and \widehat{p}_s must rescale with ε_2 . The latter is not possible, since pressures were made dimensionless on a typical value of the reduced pressure in the renal pelvis, which must be representative of the reduced pressure in the stent-ureter system at least in the neighbourhood of the kidney. We conclude that the only possibility is $B(z, t) \gg 1$, implying that the reduced pressures in the system are unfeasibly large or that the ureter is unfeasibly stretchy even under moderate pressures. We do not consider this case further.

Stiff ureter ($|K(z)| \gg 1$)

The work of §4.4 so far (excluding §4.4 above) is probably applicable for an unobstructed stented ureter, but if a section of the ureter is externally compressed (by a tumour, for example) then this section of the ureter is less easily stretched, and so the modulus of the function K is expected to be locally large; order $(1/\varepsilon_3)$, say, where for definiteness $K(0) = 1/\varepsilon_3$. We again start from the large porosity equation (4.28), and rescale the elasticity function: $K(z) = \kappa(z)/\varepsilon_3$. We then expand $B_0(z, t)$ (or $\beta_0(z, t)$) in powers of ε_3 , again assuming that $0 < \varepsilon_1 \ll \varepsilon_3$, so that the behaviour at order ε_3 can be reliably obtained using (4.28), the leading order equation in $\varepsilon_1 = 1/\Lambda$:

$$B_0(z, t) = B_{00}(z, t) + \varepsilon_3 B_{01}(z, t) + O(\varepsilon_3^2), \quad (4.53)$$

and similarly for other functions. Equation (4.27) becomes

$$\widehat{p}_{s0} = \widehat{p}_{u0} = \frac{\kappa(z)}{\varepsilon_3} (B_0(z, t) - 1), \quad (4.54)$$

from which it is clear that the leading order ureter radius must be $B_{00} \equiv 1$, since (reduced) pressures are scaled with the (reduced) pressure in the kidney and therefore must be order 1. Order $1/\varepsilon_3$ in (4.28) is then satisfied automatically, and order 1 yields

$$\frac{\partial^2}{\partial z^2} (\kappa(z) B_{10}) = 0, \quad B_{10}(0, t) = \frac{\widehat{P}_k(t)}{\kappa(0)}, \quad B_{10}(1, t) = \frac{\widehat{P}_b(t)}{\kappa(1)}. \quad (4.55)$$

(the boundary conditions come from (4.29)). Hence we have the correction to the ureter wall shape due to the slight compliance of the wall, giving the ureter shape for $|K(z)| \gg 1$ as

$$B_0(z, t) = 1 + \frac{(\widehat{P}_b(t) - \widehat{P}_k(t))z + \widehat{P}_k(t)}{K(z)} + O\left(\frac{1}{K(z)^2}\right).$$

The pressures in the stent and ureter are then linear in z to leading order,

$$\widehat{p}_{s0} = \widehat{p}_{u0} = ((\widehat{P}_b(t) - \widehat{P}_k(t))z + \widehat{P}_k(t) + O\left(\frac{1}{K(z)}\right))$$

so that the leading order flow is just Poiseuille, varying in time according to the variations in the kidney and bladder pressures. Hence if the bladder undergoes a sizeable ‘twinge’, such that the pressure rises above that in the kidney, flow will temporarily be reversed, and reflux will occur.

Small porosity

Despite the fact that the parameter Λ appears to be large for the stents we studied, it would be a simple matter to change this (punch fewer, smaller, or no holes). Furthermore, there are sometimes problems with stents fracturing in vivo, and it is conjectured by some urologists that the holes may be partly responsible for this. Hence it is worth studying the limit $\Lambda \ll 1$ to see if we can quantify the differences in the flow patterns, and draw some conclusions as to the usefulness of the holes.

We make asymptotic expansions for the functions \widehat{p}_s , \widehat{p}_u , B (and β) in powers of the small parameter Λ , as usual. Equation (4.22) for the reduced pressure in the ureter is unchanged; and for the reduced pressure in the stent, at leading order (4.23) gives \widehat{p}_{s0} varying linearly between the prescribed values at the ends:

$$\widehat{p}_{s0} = \widehat{P}_k(t) + z(\widehat{P}_b(t) - \widehat{P}_k(t)), \quad (4.56)$$

so that the leading order flow in the stent is Poiseuille. In the same way that (4.24) was derived we obtain a 2nd order nonlinear PDE for the leading order ureter shape function, which is very similar to equation (4.28) for the large porosity case:

$$8 \frac{\partial \beta_0}{\partial t} + (\beta_0 - 1)^2 \frac{\partial^2}{\partial z^2} (K(B_0 - 1)) - 2(\beta_0 \log \beta_0 - \beta_0 + 1) \frac{\partial}{\partial z} \left(\frac{\beta_0 - 1}{\log \beta_0} \frac{\partial}{\partial z} (K(B_0 - 1)) \right) = 0 \quad (4.57)$$

The boundary conditions at $z = 0, 1$ are exactly as in (4.29). We can now proceed as before, and study further simplifications to this case.

Further simplifications

As in the large porosity limit, when both end pressures $\widehat{P}_k(t)$ and $\widehat{P}_b(t)$ are equal to 1 there is a steady solution to the above model:

$$\widehat{p}_{u0} = 1 = \widehat{p}_{s0}, \quad B_0(z) = 1 + \frac{1}{K(z)},$$

probably relevant when the patient is urinating, about which we may perturb. We assume asymptotic expansions exactly as in (4.30), except that now the condition we impose on the relative sizes of the small parameters is $0 < \Lambda \ll \delta \ll 1$ (so that we can proceed beyond leading order in δ using just leading order in Λ). To order δ the pressures are then given by

$$\begin{aligned} \widehat{p}_{s0} &= 1 + \delta(\widehat{P}_{k1}(t) + z(\widehat{P}_{b1}(t) - \widehat{P}_{k1}(t))) + O(\delta^2) \\ \widehat{p}_{u0} &= 1 + \delta K(z)B_{10} + O(\delta^2). \end{aligned}$$

At order δ , analogous to equation (4.31) we obtain

$$\begin{aligned} 16B_{00}\frac{\partial B_{01}}{\partial t} &= \left(B_{00}^4 - 1 - \frac{2(B_{00}^2 - 1)^2}{\log B_{00}^2} \right) \frac{\partial^2}{\partial z^2} (KB_{01}) + \\ &2(B_{00}^2 \log B_{00}^2 - B_{00}^2 + 1) \frac{\partial}{\partial z} \left(\frac{B_{00}^2 - 1}{\log B_{00}^2} \right) \frac{\partial}{\partial z} (KB_{01}), \end{aligned} \quad (4.58)$$

which, if K is constant, simplifies to a diffusion equation analogous to (4.32):

$$\frac{\partial B_{01}}{\partial t} = E \frac{\partial^2 B_{01}}{\partial z^2} \quad E = \frac{K}{16B_{00}} \left(B_{00}^4 - 1 - \frac{2(B_{00}^2 - 1)^2}{\log B_{00}^2} \right) \equiv D - \frac{1}{16B_{00}(B_{00} - 1)} \quad (4.59)$$

The diffusion coefficient E is again always positive for $B_{00} > 1$, but exhibits very different limiting behaviour as $B_{00} \rightarrow 1^+$ to D in (4.32), since here $E \sim (B_{00} - 1)^2/12$ as $B_{00} \rightarrow 1^+$. The large B_{00} behaviour of D and E is the same; however we note that for $B_{00} > 1$ D is always strictly greater than E .

Hence we again have similarity solutions and periodic pulsing solutions exactly as investigated in §4.4, but with the new value for the diffusion coefficient.

The fluid velocities through stent and ureter are given by

$$\begin{aligned} u_s &= \frac{\delta}{4}(\widehat{P}_{b1} - \widehat{P}_{k1})(r^2 - 1), \\ u_u &= \frac{\delta K}{4} \frac{\partial B_{01}}{\partial z} (r^2 - 1 - \frac{(B_{00}^2 - 1)}{\log B_{00}^2} \log r^2) + O(\delta^2), \end{aligned}$$

hence the fluxes through stent and ureter at the bladder entrance are now given by:

$$Q_s = -\frac{\delta\pi}{8}(\widehat{P}_{b1} - \widehat{P}_{k1}) + O(\delta^2) \quad (4.60)$$

$$Q_u = -2\delta\pi B_{00}E \left. \frac{\partial B_{01}}{\partial z} \right|_{z=1} + O(\delta^2), \quad (4.61)$$

where E is defined in (4.59) above. How do these compare with the fluxes obtained for the corresponding $\Lambda \gg 1$ solutions?

Reflux for $\alpha = 0$ similarity solution

In the $\Lambda \gg 1$ limit of §4.4 we have

$$\begin{aligned} \left(\frac{-Q_s}{\delta}\right)_{\Lambda=\infty} &= \frac{1}{8}\sqrt{\frac{\pi}{Dt}}e^{-\frac{1}{4Dt}} + O(\delta), \\ \left(\frac{-Q_u}{\delta}\right)_{\Lambda=\infty} &= 2\sqrt{\frac{\pi E}{t}}B_{00}(B_{00}-1)\sqrt{\frac{E}{D}}e^{-\frac{1}{4Dt}} + O(\delta). \end{aligned}$$

In the $\Lambda \ll 1$ limit (above) we can evaluate the expressions (4.60) and (4.61) for the fluxes by replacing D by E in the $\alpha = 0$ solutions of §4.4. We find

$$\begin{aligned} \left(\frac{-Q_s}{\delta}\right)_{\Lambda=0} &= \frac{\pi}{8}\operatorname{erf}\left(\frac{1}{2\sqrt{Et}}\right) + O(\delta), \\ \left(\frac{-Q_u}{\delta}\right)_{\Lambda=0} &= 2\sqrt{\frac{\pi E}{t}}B_{00}(B_{00}-1)e^{-\frac{1}{4Et}} + O(\delta). \end{aligned}$$

Considering the reflux into the region between stent and ureter, $(-Q_u)$, at small times we have less reflux with the non-porous ($\Lambda \rightarrow 0$) stent, because

$$\sqrt{\frac{E}{D}}e^{-\frac{1}{4Dt}} < e^{-\frac{1}{4Et}} \quad 0 < t \ll 1,$$

($D > E$, remember). At large times however the situation is reversed and the non-porous stent gives greater reflux:

$$\left(\frac{-Q_u}{\delta}\right)_{\Lambda=\infty} \sim 2\sqrt{\frac{\pi E}{t}}B_{00}(B_{00}-1)\sqrt{\frac{E}{D}}, \quad \left(\frac{-Q_u}{\delta}\right)_{\Lambda=0} \sim 2\sqrt{\frac{\pi E}{t}}B_{00}(B_{00}-1).$$

The behaviour of Q_s is more complicated; but for small times we have

$$\left(\frac{-Q_s}{\delta}\right)_{\Lambda=\infty} \sim \frac{1}{8}\sqrt{\frac{\pi}{Dt}}e^{-\frac{1}{4Dt}}, \quad \left(\frac{-Q_s}{\delta}\right)_{\Lambda=0} \sim \frac{\pi}{8} - \frac{1}{4}\sqrt{\pi Et}e^{-\frac{1}{4Et}}(1 + O(t)),$$

showing that initially there is greater reflux with the non-porous stent. At large times the behaviour is:

$$\left(\frac{-Q_s}{\delta}\right)_{\Lambda=\infty} \sim \frac{1}{8}\sqrt{\frac{\pi}{Dt}}\left(1 - \frac{1}{4Dt} + O\left(\frac{1}{t^2}\right)\right), \quad \left(\frac{-Q_s}{\delta}\right)_{\Lambda=0} \sim \frac{1}{8}\sqrt{\frac{\pi}{Et}}\left(1 - \frac{1}{12Et} + O\left(\frac{1}{t^2}\right)\right).$$

Hence at large times also the reflux is greater with the non-porous stent.

The total flux over time may be found by integrating these expressions with respect to t . Clearly the integrals do not converge over infinite time, but for $t = T \gg 1$ we obtain the estimates for the integrated fluxes in the stent:

$$\int_0^T \left(\frac{-Q_s}{\delta}\right)_{\Lambda=\infty} dt \sim \frac{1}{4}\sqrt{\frac{\pi T}{D}};$$

and

$$\int_0^T \left(\frac{-Q_s}{\delta}\right)_{\Lambda=0} dt \sim \frac{1}{4}\sqrt{\frac{\pi T}{E}};$$

and for the integrated fluxes in the stent-ureter gap:

$$\int_0^T \left(\frac{-Q_u}{\delta} \right)_{\Lambda=\infty} dt \sim 4B_{00}(B_{00} - 1) \sqrt{\frac{E}{D}} \sqrt{\pi ET},$$

$$\int_0^T \left(\frac{-Q_u}{\delta} \right)_{\Lambda=0} dt \sim 4B_{00}(B_{00} - 1) \sqrt{\pi ET}.$$

Hence the total amount of fluid that has refluxed back into the stent at time $t = T \gg 1$ is clearly larger for the non-porous stent than for the porous stent. The same is true for reflux back into the gap between the stent and the ureter wall.

Reflux for $\alpha = -1/2$ similarity solution

In the limit $\Lambda \gg 1$ we find

$$\begin{aligned} \left(\frac{-Q_s}{\delta} \right)_{\Lambda=\infty} &= \frac{\pi}{16Dt} \left(1 - \int_0^{\frac{1}{4Dt}} \frac{e^{-s} ds}{\sqrt{1-4Dts}} \right), \\ \left(\frac{-Q_u}{\delta} \right)_{\Lambda=\infty} &= \frac{\pi EB_{00}(B_{00} - 1)}{Dt} \left(1 - \int_0^{\frac{1}{4Dt}} \frac{e^{-s} ds}{\sqrt{1-4Dts}} \right), \end{aligned}$$

while in the limit $\Lambda \ll 1$ the flux expressions (4.60) and (4.61) give (again using the results of §4.4 with D replaced by E):

$$\begin{aligned} \left(\frac{-Q_s}{\delta} \right)_{\Lambda=0} &= \frac{\pi}{8\sqrt{Et}} e^{-\frac{1}{4Et}} \int_0^{\frac{1}{2\sqrt{Et}}} e^{s^2} ds \equiv \frac{\pi}{8} \int_0^{\frac{1}{4Et}} \frac{e^{-s} ds}{\sqrt{1-4Ets}}, \\ \left(\frac{-Q_u}{\delta} \right)_{\Lambda=0} &= \frac{\pi B_{00}(B_{00} - 1)}{t} \left(1 - \int_0^{\frac{1}{4Et}} \frac{e^{-s} ds}{\sqrt{1-4Ets}} \right). \end{aligned}$$

For this solution it appears that the reflux into the stent is always less in the very porous limit: $(-Q_s)_{\Lambda=\infty} < (-Q_s)_{\Lambda=0}$ for all relevant values of B_{00} and t , with the large- t behaviours given by

$$\left(\frac{-Q_s}{\delta} \right)_{\Lambda=\infty} = \frac{\pi}{16} \left(\frac{1}{Dt} - \frac{1}{2D^2t^2} + O\left(\frac{1}{t^3}\right) \right), \quad \left(\frac{-Q_s}{\delta} \right)_{\Lambda=0} = \frac{\pi}{16} \left(\frac{1}{Et} - \frac{1}{6E^2t^2} + O\left(\frac{1}{t^3}\right) \right).$$

Comparing the fluxes Q_u in the limits $\Lambda = \infty$, $\Lambda = 0$, the small- t -analysis (see the comments below (4.52) in §4.4) reveals that the flux is initially in the right direction in both cases (into the bladder):

$$\left(\frac{Q_u}{\delta} \right)_{\Lambda=\infty} = 2\pi B_{00}(B_{00}-1)E(1+6Dt+O(t^2)), \quad \left(\frac{Q_u}{\delta} \right)_{\Lambda=0} = 2\pi B_{00}(B_{00}-1)E(1+6Et+O(t^2)),$$

the case $\Lambda = \infty$ giving a larger flux into the bladder. The large- t behaviours of these fluxes Q_u satisfy:

$$\left(\frac{-Q_u}{\delta} \right)_{\Lambda=\infty} = \frac{\pi B_{00}(B_{00} - 1)}{Dt} \left(E - \frac{E}{2Dt} + O\left(\frac{1}{t^2}\right) \right),$$

$$\left(\frac{-Q_u}{\delta}\right)_{\Lambda=0} = \frac{\pi B_{00}(B_{00} - 1)}{Dt} \left(D - \frac{D}{2Et} + O\left(\frac{1}{t^2}\right)\right).$$

This demonstrates that at large times there is less reflux into the stent-ureter gap in the limit $\Lambda = \infty$ (for these particular similarity solutions). Since the form of this large- t flux is $O(1/t)$, it follows that the time-integrated total (re)flux from $t = 0$ to $t = T$ must be order $\log T$ for $T \gg 1$, the larger total reflux being observed for the non-porous stent.

These simple examples indicate that holes in the stent are desirable, in that they appear to inhibit reflux.

Stiff ureter $|K(z)| \gg 1$

We proceed as in §4.4, writing $K(z) = \kappa(z)/\varepsilon_3$ and asymptotically expanding the functions B_0 , β_0 , \hat{p}_{u0} , \hat{p}_{s0} in powers of ε_3 as in (4.53). From equation (4.22) which still holds here we again find $B_{00} = 1$ at leading order, giving the leading order pressure in the ureter as $\hat{p}_{u00} = \kappa(z)B_{10}$. The stent pressure is still given by (4.56). The higher order behaviour is different from that of the porous stent: substituting the asymptotic expansions into (4.57) we find

$$16\varepsilon_3 \frac{\partial B_{10}}{\partial t} + 8\varepsilon_3^2 \frac{\partial}{\partial t}(2B_{20} + B_{10}^2) + \dots = 4\varepsilon_3^2 B_{10}^2 \frac{\partial^2}{\partial z^2}(\kappa(z)B_{10}) + \dots \quad (4.62)$$

This suggests rescaling time with $1/\varepsilon_3$: $t = \tau/\varepsilon_3$; at order ε_3^2 (4.62) then gives the diffusion-type equation

$$4 \frac{\partial B_{10}}{\partial \tau} = B_{10}^2 \frac{\partial^2}{\partial z^2}(\kappa(z)B_{10}).$$

For $B_0 = 1 + \varepsilon_3 B_{10}$ to give a valid approximation to the ureter radius $B = B_0 + O(\Lambda)$ we require $0 < \Lambda \ll \varepsilon_3$. The boundary conditions on B_{10} come from (4.29):

$$B_{10}(0, \tau) = \frac{\hat{P}_k(\tau)}{\kappa(0)}, \quad B_{10}(1, \tau) = \frac{\hat{P}_b(\tau)}{\kappa(1)}.$$

We do not pursue this model further in this report.

4.5 Experimentally Determining the Porosity of Ureteric Stents

An attempt was made to determine the porosity of a ureteric stent experimentally, since this variable is important in any theoretical analysis. The design of the stent is shown in Figure 6. The ultimate aim of the experiment was to obtain an order of magnitude estimate of the porosity parameter for the stent, the ratio of the flux per unit area through the stent wall to pressure difference across the stent wall. Define $\lambda^* = k^*/\mu^*$ where k^* is the permeability of the stent wall and μ^* is the viscosity of the fluid used. The flux per unit area will be described as Q^* , while the pressure difference across the tube surface will be Δp^* . Then Darcy's Law gives

$$\lambda^* = \frac{q^*}{\Delta p^*}. \quad (4.63)$$

(cf (4.9) and (4.11)). The relevant dimensionless parameter Λ governing the importance of porosity (more precisely the ratio of fluid transfer across the tube to the fluid transfer out of the end of the tube) was given in (4.17) by

$$\Lambda = \frac{16\lambda^* L^{*2} \mu^*}{a^{*3}}, \quad (4.64)$$

where L^* is the length of the stent and a^* the radius.



Figure 6: Schematic sketch of a ureteric stent

4.5.1 Experimental Setup

Before setting up the experiment the effect of the ends of the stent was considered. They have a “J” style shape, which is a loop (of radius of approximately 5 mm), as illustrated in Figure 7. These are used to anchor the stent in the kidney and the bladder. A syringe was attached to the end of the loop at one end of the stent and dyed fluid was forced into the stent. It was observed that almost all the fluid left the stent through the holes in the loop itself, regardless of the pressure applied to the syringe plunger. It was accepted that the loop provides so much resistance to the flow that urine enters the tube through the holes in the loop *in vivo*, rather than the larger hole in the end of the stent. Since the aim of the experiments was to find the porosity of the middle straight part of the stent, the ends of the tube were straightened for the experiments.

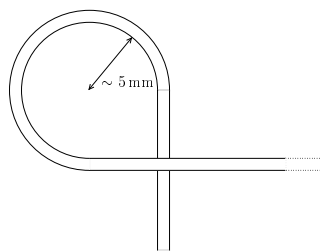


Figure 7: The design of the end of a “J” type stent

A 50ml syringe was attached to one of the straightened ends of the ureteric stent. The stent was placed in a fluid (water) filled plastic bottle (of volume 1 L) placed on its side. The needle of the attached syringe was pushed through the bunged entrance to the bottle. The bottle was not completely filled with water, so there was an air pocket at the top of the bottle (see Figure 8) and this was perforated so that the air pressure remained atmospheric. This arrangement was used to approximate the pressures in the

ureter, as it is naïve to assume the porosity is independent of the absolute pressures and other external parameters of its environment. Warm water was used ($\sim 25^\circ\text{C}$) to mimic *in vivo* conditions.

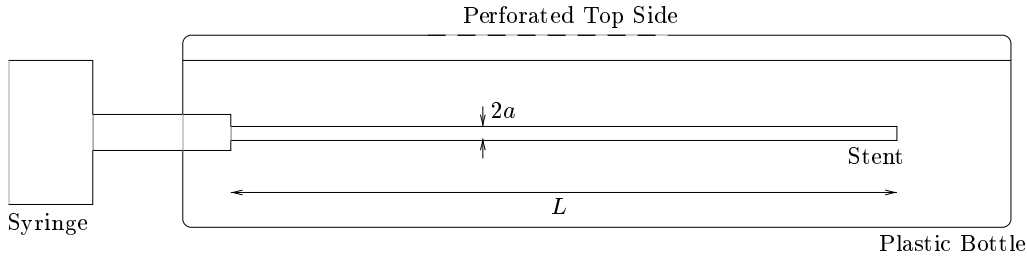


Figure 8: Experimental setup

The aim was to time how long it takes for a fluid to flow from the syringe to the ambient water in the bottle.

4.5.2 The First Experiment

The first attempt at measuring the time taken to pass fluid through the system was done at a pressure difference (of the syringe to the tube) similar to that in the ureter (approximately $20 - 50 \text{ cm H}_2\text{O}$). This was easily achieved by removing the plunger from the syringe and holding it 20 cm above the stent to create a hydrostatic pressure difference of $20 \text{ cm H}_2\text{O}$). The syringe was filled with 50 ml of water dyed with water soluble blue ink solution, that showed no indication of diffusion. After the experiment the dye was not seen to spread outwards for several minutes. The dyed fluid was completely transferred to the outside of the tube after passing through the first couple of holes in the tube. The holes are spaced at two per cm and, including those on the end curls, there are a total of 60 holes in the stent.

4.5.3 The Second Experiment

In an attempt to arrange a system in which fluid reached the end of the tube it was necessary to apply a larger force manually by replacing the plunger to the syringe and using it to exert higher pressures than $20 \text{ cm H}_2\text{O}$. When this was performed the dyed fluid passed through all the holes (just reaching the end of the tube). The results are presented in Table 1.

Volume(ml)	30	50	50	50
Time (sec)	15.91	27.67	26.32	26.97
Volume Flux (ml/sec)	1.89	1.81	1.90	1.85

Table 1: Experimental Results

It can be seen that volume flux rates in all cases are similar (and close to *in vivo* values). This is important since it implies a similar force is applied to the plunger every time. The Reynolds number of the flow can also be calculated. The velocity is about 1.0 cm s^{-1} through the holes in the stent, with a lengthscale of about 0.1 cm, giving a Reynolds number of

$$\text{Re} \approx 10, \quad (4.65)$$

with a similar Reduced Reynolds number (since the lengthscales are about the same—the holes have a diameter of similar size to the thickness of the stent). The Reynolds number is taken using the lengthscale of the distance travelled (the tube thickness), whereas the Reduced Reynolds number uses the radius of the hole as a lengthscale.

4.5.4 Calculation of the Porosity Parameter

Two methods can be used to calculate λ^* . The first is a standard method, which assumes that flow through the holes is at low Reynolds number, however from equation (4.65) this is not appropriate and furthermore there was difficulty in acquiring the required measurements. It was thought that a more *ad hoc* method could be used, that was far simpler to execute. It is a high Reynolds number method, which is not unreasonable given the estimate stated in equation (4.65).

Traditional Low Reynolds Number Method

Assuming that the flow through a single hole is Poiseuille, the velocity is given by,

$$u^*(r^*) = \frac{1}{4\mu^*} G^* (r^{*2} - e^{*2}), \quad (4.66)$$

where G^* is the negative pressure gradient, e^* is the radius of a hole and $u^*(r^*)$ is the velocity perpendicular to the stent wall. Integrating equation (4.66) across the area of the hole gives the volume flux through an individual hole, $q^{*(1)}$, as

$$q^{*(1)} = -\frac{\pi}{8\mu^*} G^* e^{*4}. \quad (4.67)$$

There are 60 holes regularly distributed along the $L^* = 30 \text{ cm}$ tube. So assuming that there is no flow through the hole at the end of the stent (which was confirmed by observation) means that $q_{tot}^* = 60q^{*(1)}$, where q_{tot}^* is the total volume flux, as given in Table 1. If the pressure gradient is constant within the interior of a hole (i.e. $G^* = -\Delta p^*/h^*$), then

$$\Delta p^* = \frac{2}{15} \frac{q_{tot}^* \mu^* h^*}{\pi e^{*4}}. \quad (4.68)$$

The flux per unit area is given by

$$Q^* = \frac{q_{tot}^*}{2\pi a^* L^*}. \quad (4.69)$$

Thus from equation (4.63) λ^* can be estimated as

$$\lambda^* = \frac{15e^{*4}}{4\mu^* a^* L^* h^*}, \quad (4.70)$$

and the appropriate parameter (4.64) can be found,

$$\Lambda = \frac{60e^{*4}L^*}{a^{*4}h^*}. \quad (4.71)$$

This parameter illustrates some fairly intuitive results. Increasing the radius of the holes increases the porosity. Likewise decreasing the radius of the tube, or decreasing its thickness also increases porosity (as was suggested by one of the included experimental papers).

Measuring e^* and h^* accurately was not possible, so it was necessary to take advantage of the relatively high Reynolds number, (4.65), to find a measure of the porosity.

A More *Ad Hoc* Method

It is assumed that the fluid flows out of the stent at the same rate per unit area down the tube (i.e. Q^* is constant) and that the fluid is approximately static just before it leaves the tube (i.e. when it is very close to the wall). The latter assumption seems valid as the fluid is observed to flow out of the stent in a direction perpendicular to the stent. Under these conditions one can use the steady Bernoulli theorem on a streamline (from just in the tube where the fluid velocity is nearly zero near the tube wall, to just outside where the flow is perpendicular to the tube wall),

$$\frac{1}{2}\rho^*\bar{u}^{*2} = \Delta p^*, \quad (4.72)$$

where \bar{u}^* is the velocity of the fluid leaving the tube. Thus an expression for λ^* can be found, from its definition in equation (4.63),

$$\lambda^* = \frac{2Q^*}{\rho^*\bar{u}^{*2}}. \quad (4.73)$$

Furthermore mass conservation demands that,

$$2\pi a^*L^*Q^* = 60\pi e^{*2}\bar{u}^*. \quad (4.74)$$

This provides an expression for the porosity,

$$\lambda^* = \frac{1800e^{*4}}{\rho^*a^{*2}L^{*2}Q^*}. \quad (4.75)$$

Since Q^* is constant, $2\pi a^*L^*Q^* = \mathcal{V}^*$, where \mathcal{V}^* is the volume flow rate from the syringe (here it should be noted that only small amounts of fluid flow out of the end of the tube relative to the amounts coming from any of the holes in the side of the tube). Thus,

$$\lambda^* = \frac{4\pi a^*L^*}{\rho^*\mathcal{V}^*}. \quad (4.76)$$

Taking $L^* = 30$ cm and $a^* = 0.1$ cm gives a value of λ^* :

$$\lambda^* \approx 1800 \left(\frac{e^*}{a^*} \frac{e^*}{L^*} \right)^2 \text{ m}^2 \text{ s kg}^{-1}, \quad (4.77)$$

where the arithmetic mean of the value for \mathcal{V}^* is used from Table 1.

4.5.5 Parameter Estimation

Using equation (4.77) it is possible to make an estimate of the porosity parameter defined in equation (4.64), which is found to be

$$\Lambda = 2 \times 10^7 \left(\frac{e^*}{a^*} \frac{e^*}{L^*} \right)^2. \quad (4.78)$$

Assuming $e^*/a^* \approx 0.5$ and $e^*/L^* \approx 2 \times 10^{-2}$ for a hole diameter of approximately 0.5 mm,

$$\Lambda \approx 20. \quad (4.79)$$

This means that the tube is quite porous and far from using a low porosity limit model that was intuitively thought to model the physical system the converse is true: a high porosity limit must be taken. This has repercussions for the modelling of the flow through the ureter and stent from the kidney to bladder. It is also important for understanding *reflux* where a short burst of high pressure from the bladder (as it evacuates or has a “twinge” due to irritation caused by the end of the stent) can cause flow in the opposite direction, carrying bacteria rich urine back from the bladder to the kidney.

If the Low Reynolds number method is used the result is much higher ($\Lambda \approx 1100$ for a hole depth of $h^* = 0.1$ cm), but for reasons discussed earlier, it would be naïve to just accept this as the parameter value.

4.6 Conclusions

In this report we have used simplified mathematical models to study the fluid dynamics of a stented ureter, with the goal of answering the four questions set out at the end of §4.1.

The issue of stent encrustation was briefly considered in §4.2. Without detailed analysis it was concluded that the main reason for encrustation occurring is that the end curls of the stent are situated in nearly stagnant urine (in the widest parts of the renal pelvis and bladder). Assuming that a faster shear flow past the stent surface would mean less encrustation over a given time period, we suggested changing the design so that, if possible, the whole of the stent lies in regions of appreciable flow speed. Whether or not our suggestion is clinically practical remains to be seen, however.

In §4.3, very basic models (assuming Poiseuille flow) were used to derive estimates of the time taken for urine to reflux back along the entire length of the ureter to the kidney, in situations where the bladder pressure is raised above that in the renal pelvis. This was done for two extreme cases: a stent with no holes, and a stent that is extremely porous (*e.g.* a very fine wire mesh tube). These simple estimates led us to conclude that while there may be some degree of reflux during a bladder twinge, the short duration of the twinge means that urine is unlikely to reflux all the way back to the bladder. During urination however, which can last much longer (and which involves a larger negative pressure differential), total reflux may well occur.

We then went on to formulate a more complicated mathematical model, which treats the ureter as an elastic walled tube, with a rigid porous tube (the stent) inside it. Cylindrical symmetry was assumed, which will of course not be the case in practice. The small aspect ratio of the system enabled us to use lubrication theory to derive explicit evolution equations for the pressures within the stent and ureter, and for the ureter radius

$B(z, t)$. Since these evolution equations are very complicated, we then set about making various asymptotic simplifications. In particular, we again considered the cases of high- and low-porosity stents, to see if we could draw any conclusions about the effect of the holes on the flow. Regarding the reflux issue, which is the major focus of our study, in the two test solutions to our model that we studied it appeared that the holes reduce reflux. Since the holes may also serve a useful purpose in the neighbourhood of the blockage, it seems they are a good design feature.

During the Study Group several experiments were carried out to determine the porosity of a JJ-stent. The results of these experiments are presented in §4.5, and the conclusions agree with what we expect from the mathematics alone.

References

- [1] Dauleh, M.J., Byrne, D.J., Baxby, K. (1995) Non-refluxing minimal irritation ureteric stent. *British Journal of Urology* **76**.